

FORMATION OF Al-Zn-Si COATINGS ON LOW CARBON STEEL SUBSTRATES

Yvonne Durandet¹, Les Strezov², Nick Ebrill³

¹ BHP Research - Melbourne Laboratories, 245 Wellington Rd, Mulgrave, Vic. 3170, Australia

² BHP Research - Newcastle Laboratories, Off Vale St, Shortland, NSW 2307, Australia

³ University of Newcastle, Dept of Chemical Engineering, University Dve, Callaghan, NSW 2308, Australia

Synopsis : The formation of interfacial layers during the initial stages of solid-liquid contact in hot dip coating was simulated by a laboratory dip testing technique. The dipping apparatus enabled the steel substrate to be preheated to the desired temperature under controlled atmosphere, then dipped in the coating melt for immersion times as low as 20 milliseconds. Results of dipping experiments of thin low-carbon steel strips in iron-saturated melt of 55wt% Al - 43.4wt% Zn - 1.6wt% Si alloy are presented. It is shown that the strip preheat temperature had a profound influence on the kinetics of the formation of the alloy layer, the nature of the interfacial phases and the surface appearance of the outer free coating. Mechanisms for the formation of the alloy layer and nucleation and growth of the overlay are proposed.

Key words : Al-Zn coating ; Initial Contact ; Interfacial Alloy Layer ; Intermetallic Phases ; Nucleation ; Growth ; Spangles ; Solidification.

1. Introduction

Little has been published on the formation of the alloy layer during the initial stages of solid-liquid contact in hot dip coating, except for studies on the wetting of coating alloys on steel substrates under isothermal conditions^[1].

Most laboratory studies of the alloy layer formation in 55%Al-Zn hot dip coatings have been performed at dipping times greater than 3s^[2-4]. Fluxes were used to prevent oxidation of the steel surface prior to dipping and required about 3 to 5s to be dispersed in the coating melt. In addition, no pre-heating was applied to the steel substrate, except when drying the fluxes at 80-120°C, so that the initial temperature difference between the substrate and the melt was of the order of 480-530°C, compared to 60-160°C in production environment. A transient period of 2-3s was reported for a 0.6mm thick steel strip to reach a bath temperature of 610°C^[2]. Beyond 3s dipping time, steady state conditions were established and the alloying reaction occurred isothermally at the bath temperature.

More recently, strip immersion times of less than 1s and initial pot-strip temperature differences of less than 140°C have been achieved using a modified pilot coating line with a bath of 55%Al-Zn composition^[5]. A continuous alloy layer was observed for contact times as low as 0.27s. Bath temperature variations of 600 to 620°C were reported to have more influence on the alloy growth kinetics than strip temperature

variations of 480 to 520°C^[6]. At immersion times of 0.3 to 4s and strip preheat temperatures lower than the melt, the alloy layer consisted of α -Fe₅Si₂Al₂₀^[2,5]. At longer immersion times of about 60s, additional phases of θ -FeAl₃ and η -Fe₂Al₅ were present^[4].

The present work was undertaken to investigate the influence of substrate preheat temperature on the formation of Al- 43.4Zn- 1.6Si coatings on low carbon steel strip, with particular emphasis on very short immersion times.

2. Experimental Conditions and Procedure

Dip coating experiments were conducted without fluxes using the laboratory dip tester at BHP Research, Newcastle, whose vertical dipping motion design enabled a minimum immersion time in the melt of 0.08s^[7-8]. The equipment was modified to enable preheating of the substrate up to 800°C under a reducing atmosphere (Fig. 1). Immersion times as low as 0.02s were achieved with a rotating motion of the substrate through the melt by fitting the leading end of the dipping rack with a small gearbox.

The coating bath was prepared by melting under argon atmosphere the appropriate proportions of high purity Al, Zn and pre-alloyed Al-12wt% Si charges, and saturated with Fe (Table 1). The bath temperature was continuously monitored and maintained at 610±3°C under argon atmosphere, using a type-K thermocouple fitted inside an alumina tube immersed in the melt.

Cold rolled low carbon steel strip coupons (Table 1) of 0.4mm thickness (x 60mm width x 150mm length) were used as substrates. The coupons were first degreased and rinsed ultrasonically in alcohol, and cloth-wipe cleaned with a naphtha based solvent. Before attaching a coupon onto the dipping paddle, its surface was mechanically cleaned with a 1200 mesh emery paper, then ultrasonically cleaned in alcohol and air-dried. The strip preheat temperature was monitored using a type-K thermocouple attached to the coupon's surface.

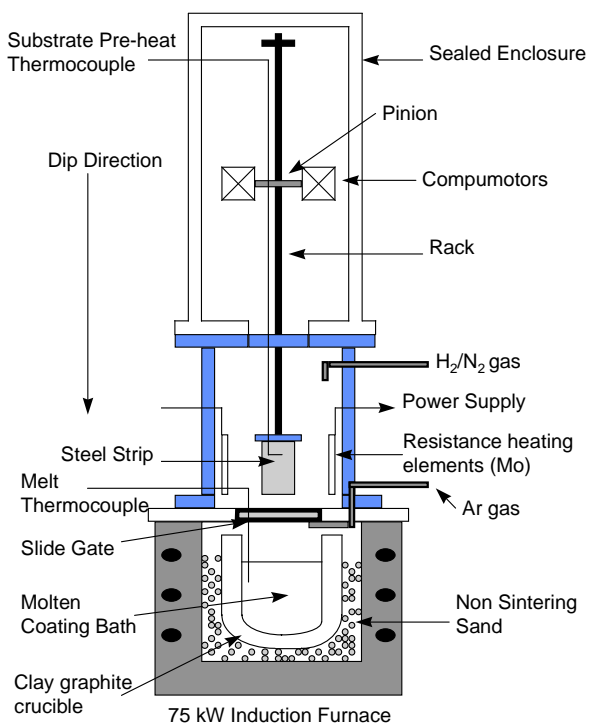


Figure 1 : Schematic of experimental apparatus.

The dip tester enclosure was flushed with argon to reduce the oxygen level to below 0.2%. A gas mixture of 5% hydrogen in nitrogen was used during preheating. Typical oxygen levels during substrate preheating were of the order of $10^{-18}\%$.

The slide gate separating the atmosphere chambers of the melting furnace and the dip tester was opened just before dipping. After dipping and as soon as the paddle returned to its home position, the slide gate was closed and the coated strip was cooled with argon to temperatures below 300°C before detaching (pneumatic clamp) the dip tester from the melting furnace.

The experimental variables included strip immersion time in the melt (0.02 to 0.3s) and strip preheat temperature (480 to 700°C, i.e. the initial melt-strip temperature difference varied from -90°C to +130°C).

Table 1 : Steel Substrate and Melt Composition in weight percentage (wt%)

Strip Coupon		Melt	
C	0.055	Al	53.2 - 54.8
P	0.01	Zn	43.2 - 44.8
Mn	0.24	Si	1.5 - 1.6
Si	0.005	Fe	0.39 - 0.46
S	0.013	Ti	0.013 - 0.016
Al	0.04	Total others < 0.02	
N	0.0042		

Examination of the coating surface and internal microstructure was carried out using light optical and scanning electron microscopy (JEOL JSM 6300F fitted with a Noran EDS Germanium detector).

Measurements of alloy layer thickness were made on longitudinal sections (i.e. parallel to the dipping direction) to account for variations of immersion time with position along the strip length due to the dipping motion. Samples were prepared using standard metallographic techniques and etched with Nital.

Concentration profiles through the coating were obtained by Xray-EDS analysis in a Philips SEM505.

The determination of alloy layer phases was performed by the Australian Key Centre for Microscopy and Microanalysis at the University of Sydney using Xray-EDS and electron diffraction analyses in a Philips EM 430 and CM12 TEM.

3. Results

3.1. Coating Overlay

The surface appearance of the dip test samples generally displayed larger spangles towards the leading (bottom) edge of the strip where accumulation of the liquid overlay occurred upon withdrawal from the bath (Fig. 2). However, the effect of strip preheat temperature was evinced by a profound reduction in spangle size with increasing preheat temperature.

The overlay microstructure was similar although coarser than that of production environment due to lower cooling rates after dipping. It consisted essentially of Al-rich primary dendrites, Zn-rich microsegregation and interdendritic Si phases. Through thickness concentration profiles showed the presence of Zn enrichment at the alloy layer-overlay interface (Fig. 3), as reported elsewhere^[9].

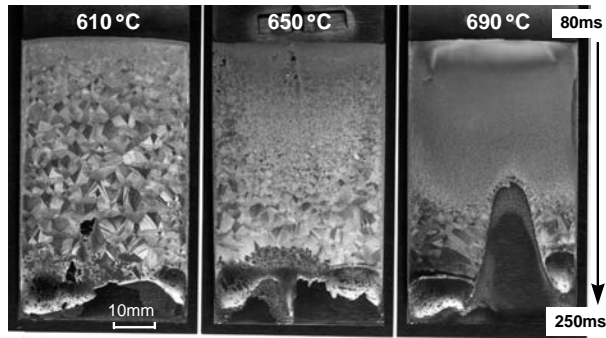


Figure 2 : Effect of strip preheat temperature on the surface appearance of the coating.

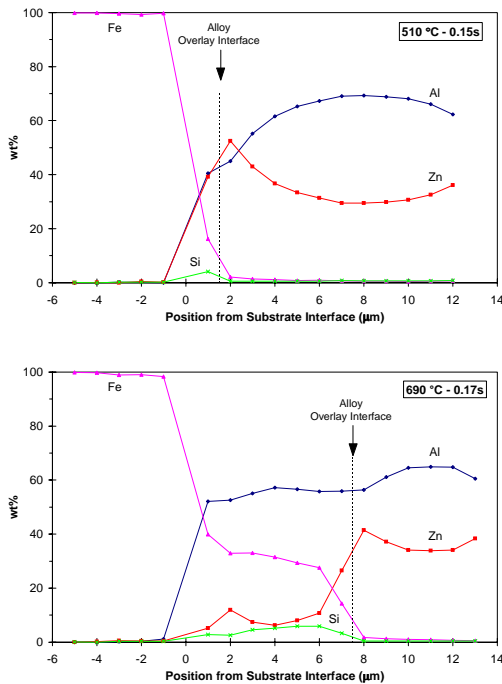


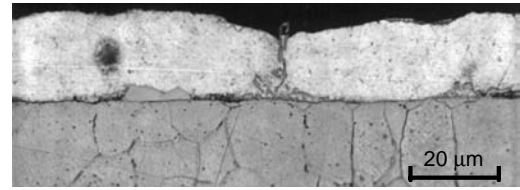
Figure 3 : Concentration profiles showing the presence of Fe-Al alloy layer and Zn segregation at the alloy layer-overlay interface

3.2. Alloy Layer

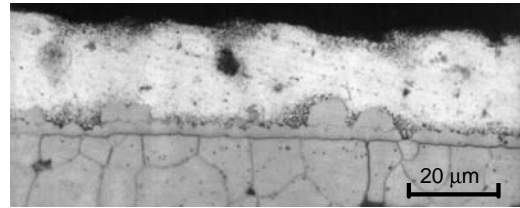
The effect of strip preheat temperature was also evident at the strip-overlay interface where the interfacial layer was thicker and more uniform with increasing strip preheat temperature (Fig. 4).

As expected, the thickness of the interfacial alloy layer increased with increasing dipping time. Most striking was the profound influence of the strip preheat temperature on the growth rate of the alloy layer (Fig. 5).

Concentration profiles showed that the interfacial layer consisted of Fe-Al alloy phases with some Si and Zn (Fig. 3). Trends in the distribution of Fe through the steel-coating interface confirmed the influence of immersion time and strip preheat temperature on the alloy layer formation (Fig. 6).



Non uniform interfacial layer (510 ± 10°C strip preheat)



Uniform interfacial layer (690 ± 10°C preheat)

Figure 4 : Effect of strip preheat temperature on the appearance of the alloy layer (0.02s immersion time).

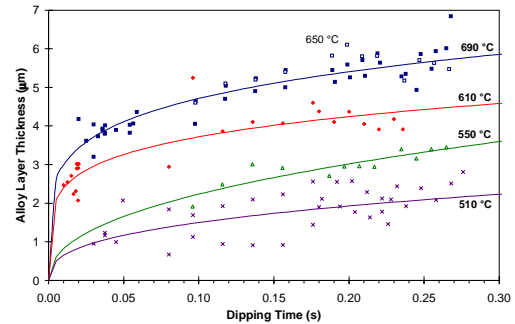


Figure 5 : Effect of strip preheat temperature on the alloy layer growth at short immersion times.

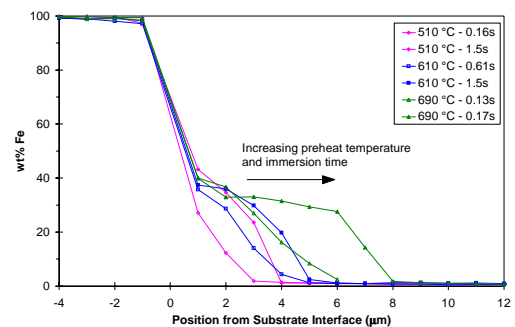


Figure 6 : Effect of strip preheat temperature and immersion time on Fe distribution through the alloy layer.

Intermetallic phases found in the alloy layer are given in Table 2. The occurrence of those phases and their relative distribution varied with strip preheat temperature and immersion times.

Table 2 : Summary of intermetallic alloy phases

Phase	Structure	Lattice Parameters (± 0.06 nm)		
		a	b	c
Fe ₂ Al ₅ η -phase	c-centred orthorhombic	0.8	0.65	0.44
FeAl ₃ θ -phase	c-centred monoclinic	1.24- 1.62	1.56- 1.62	1.26- 1.29
Fe ₅ Si ₂ Al ₂₀ α (τ_5) phase	bcc	1.24-1.3		

The η -phase appeared essentially as horizontally elongated grains directly adjacent to the steel surface, either as isolated grains or a continuous layer (Fig. 7-8). It was the only phase found to have common orientation relationships with the substrate [10]. The θ -phase occurred as a layer of columnar grains above the η -phase or the steel surface (Fig. 7-8). The α -phase generally occurred at the alloy layer-overlay interface as a layer above the θ -phase layer and as large isolated prismatic grains (Fig. 8). Prismatic α -grains were also observed within the overlay and occasionally at the steel surface where the alloy layer was discontinuous. Some θ -phase precipitates were also found in the α -phase layer at low preheat temperature.

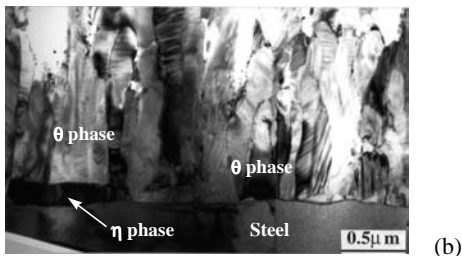
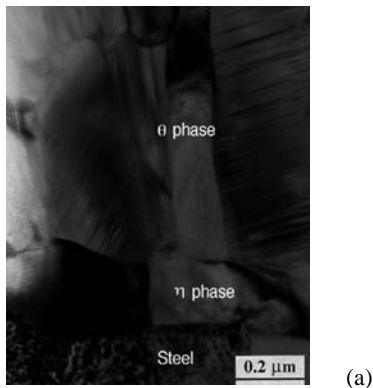


Figure 7 : Occurrence of η -Fe₂Al₅ and θ -FeAl₃ phases at 80-250ms immersion time at (a) 690°C and (b) 510°C strip preheat temperature [10].

At immersion times of less than 0.1s, the Fe content of the intermetallic phase directly adjacent to the substrate increased significantly with increasing strip preheat temperature while the Al content was comparatively little affected (Fig. 9).

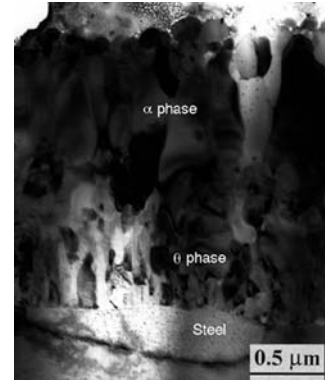


Figure 8 : Occurrence of θ -FeAl₃ and α -Fe₅Si₂Al₂₀ phases at 510°C strip preheat temperature and 80-250ms immersion time [10].

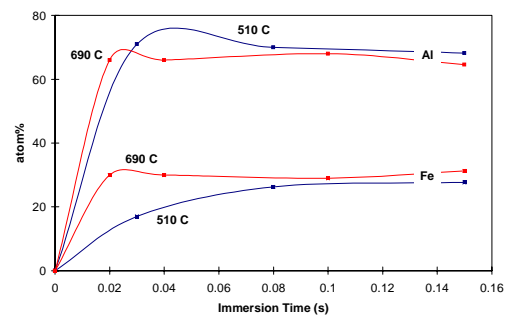


Figure 9 : Effect of strip preheat temperature and immersion time on the Fe and Al content of the intermetallic phase directly adjacent to the steel surface.

4. Interpretation of Results and Discussion

4.1. Alloy Layer Formation

Intermetallic alloy phases found in the present study were those suggested by the binary Fe-Al and ternary Fe-Al-Si alloy phase diagrams. Indeed, their occurrence is thermodynamically possible since there is little difference in their free energy of formation^[11-12]. However, at short immersion times, kinetic factors such as transient heat and mass transfer conditions prevail. The alloying reaction becomes interface controlled and deviations from parabolic to linear growth kinetics could be expected^[13]. The initial conditions at the solid-liquid interface can therefore be expected to influence the nature and sequence of formation of the intermetallic alloy phases^[14].

In the present study, competitive nucleation and growth kinetics of those phases were affected by varying the initial strip entry temperature. Results indicate that increasing the strip preheat temperature increased the mobility of Fe at the substrate-coating interface (Fig. 9). Calculations of diffusion coefficients from concentration profiles showed that the growth kinetic of the overall alloy layer was thereafter determined by the diffusion of Fe through the intermetallic layer (Fig. 10). Increasing the strip preheat temperature from 510 to 690°C increased the rate of Fe diffusion through the FeAl₃ phase by a factor of ten, leading to the observed increases in alloy layer thicknesses.

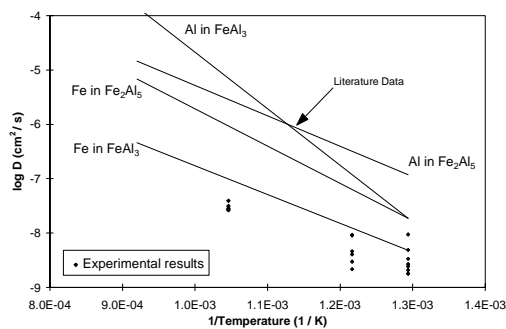


Figure 10 : Diffusion of Fe in the various phase layers (Arrhenius plots derived from literature data^[13]).

It is proposed that the first intermetallic phase to form at the initial stages of solid-liquid contact is the FeAl₃ phase. The development of subsequent intermetallic phases is then controlled by the diffusion of Fe from the substrate through this initial phase. The build-up of Fe at the substrate-FeAl₃ interface can then lead to the formation of Fe₂Al₅, growing epitaxially on the substrate, to establish local equilibrium at the strip-alloy layer

interface. At the FeAl₃-liquid interface, the local equilibrium is attained by the formation of the Fe₅Si₂Al₂₀ phase. This is consistent with the experimental results where the predominant phase at the steel-alloy layer interface, at low strip preheat temperature, is FeAl₃ (Fig. 7b). At high strip preheat temperature, the phase adjacent to the strip is Fe₂Al₅ with FeAl₃ above (Fig. 7a).

4.2. Solidification of Overlay

It has been suggested that the formation of spangles during solidification of the overlay may occur by heterogeneous nucleation at the alloy layer surface, within or at the overlay surface^[15-17]. In the present study, the occurrence of Zn microsegregation, Si phases and large faceted α -Fe₅Si₂Al₂₀ grains at the alloy layer-overlay interface (Fig. 3, 8) indicates that solidification proceeded towards, rather than from, the alloy layer surface. Modeling of the heat transfer between the strip and the entrained liquid layer^[18] showed that after the bath exit, the outer surface of the liquid layer was always colder than the strip, suggesting that subsequent solidification will proceed from the outer coating surface towards the strip. Under such conditions, the nucleation of the Al-rich dendrites would have to occur at the free surface. Detailed examination of the coating surface revealed the presence of intermetallic particles at the centre of spangles (Fig. 11).

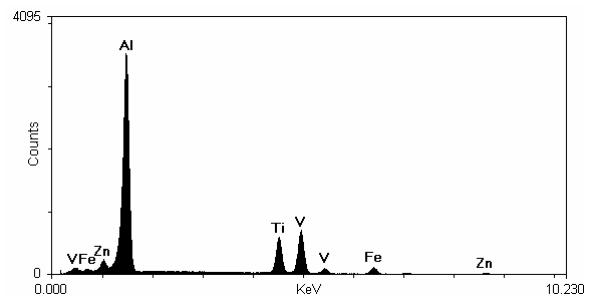
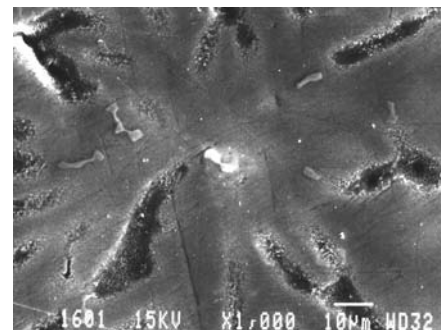


Figure 11 : Al-(Ti,V,Fe) [white particle] intermetallic phase formed initially at the coating surface during solidification of the overlay (grey particles are Al-Fe).

The first solid phases of Al-rich intermetallics precipitate from the melt at the free surface on cooling. These provide the sites for heterogeneous nucleation of primary Al-Zn dendrites. Subsequent

growth of the surface dendrites proceeds radially by constitutional supercooling along preferential crystallographic orientation, leading to the formation of the so-called spangles. Secondary or tertiary dendrite arms grow through the overlay thickness by thermal undercooling. The proposed mechanism is schematically represented in Fig. 12.

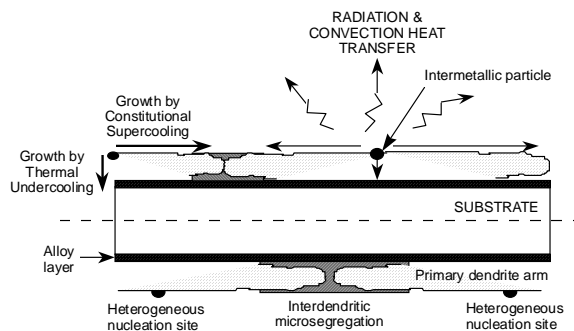


Figure 12 : Schematic diagram of the proposed mechanism for the solidification of the overlay.

The observed reduction in spangle size (Fig. 2) with increasing strip preheat temperature can therefore be attributed to increased nucleation density at the free surface. At high strip preheat temperature, the temperature of the entrained liquid boundary layer increases, locally increasing the solubility of Fe and other metallic impurities. At the bath exit, precipitation of Al-rich intermetallics occurs upon cooling of the liquid overlay.

5. Acknowledgments

The authors would like to express their gratitude to Dr J. Herbertson, General Manager, of BHP Steel and Dr G. Belton, Chief Scientist, of BHP Research for their encouragements and guidance. We would like to thank Professor M. Rappaz and Mr A. Semoroz of Ecole Polytechnique Federale de Lausanne, Switzerland, for conducting the heat transfer modeling, and Professor D. Cockayne and Dr J. Zou of the University of Sydney for the TEM analysis. The valuable contribution of our colleagues from the University of Newcastle is also gratefully acknowledged. Finally, we are thankful to BHP for permission to publish this article.

6. References

- 1 A.A. Tarasova and A.Y. Novozhilov, *Adgez. Rasplavov Paika Mater*, 11 (1983), p. 24-26.
- 2 J.H. Selverian, A.R. Marder and M.R. Notis, *Metall. Trans. A*, 19A (1988), p. 1193-1203.
- 3 J.H. Selverian, A.R. Marder and M.R. Notis, *Metall. Trans. A*, 20A (1989), p. 543-555.
- 4 P.D. Mercer, *Proc. Inter. Conf. Physical Metallurgy of Zinc Coated Steel*, San Francisco, California (1993), p. 129-135.
- 5 Z.F. Zhou, G.M. Tilden, Q.Y. Liu, P.D. Mercer and D.J. Willis, *Conf. Proc. Galvatech '95*, Chicago, IL (1995), p. 289-293.
- 6 G.M. Tilden, G.C. Warner and D.J. Willis, *BHP Coated Steel Research Laboratories, Private Communication* (1995).
- 7 L. Strezov, PhD Thesis (1994), 'Interfacial Heat Transfer Mechanisms Associated with the Direct Contacting of Copper Substrates by Liquid Stainless Steel', The University of Newcastle.
- 8 L. Strezov and J. Herbertson, Submitted ISIJ (1998), 'Experimental Studies of Interfacial Heat Transfer and Initial Solidification Pertinent to Strip Casting', To be published.
- 9 H.J. Cleary, *Microstructural Science*, 12 (1985), p. 105-113.
- 10 J. Zou, X.Z. Liao, X.F. Duan, Y. Durandet and D.J.H. Cockayne, *Proc. 14th Inter. Congress Electron Microscopy*, Cancun, Mexico (1998).
- 11 V.R. Ryabov, National Bureau of Standards, Report No. PB86-205242/WMS (1985).
- 12 E.G. Ivanov, *Met. Sci. Heat Treat. (USSR)*, 21 (5-6) (1979), p. 449-452.
- 13 R.W. Richards, R.D. Jones, P.D. Clements and H. Clarke, *International Materials Reviews*, 39 (5) (1994), p. 191-212.
- 14 Y. Lepetre, J.M. Montaigne, M. Guttman and J. Philibert, *Proc. Inter. Symp. On Zinc-based Steel Coating Systems : Production and Performance*, San Antonio, Texas (1998), Publ. TMS, p. 95-106.
- 15 H. Klang and R. Kiusalaas, *3rd Inter. Conf. on Solidification Processing*, Sheffield, England (1987), p. 327-330.
- 16 F. Weinberg, *Proc. F. Weinberg Inter. Symp. on Solidification Processing*, Hamilton, Ontario (1990), p. 3-11.
- 17 F.A. Fasoyinu and F. Weinberg, *Metall. Trans. B*, 21B (1990), p. 549-558.
- 18 A. Semoroz and M. Rappaz, EPFL Switzerland, Private Communication (1997).